

NJC

Accepted Manuscript



This is an *Accepted Manuscript*, which has been through the Royal Society of Chemistry peer review process and has been accepted for publication.

Accepted Manuscripts are published online shortly after acceptance, before technical editing, formatting and proof reading. Using this free service, authors can make their results available to the community, in citable form, before we publish the edited article. We will replace this *Accepted Manuscript* with the edited and formatted *Advance Article* as soon as it is available.

You can find more information about *Accepted Manuscripts* in the [Information for Authors](#).

Please note that technical editing may introduce minor changes to the text and/or graphics, which may alter content. The journal's standard [Terms & Conditions](#) and the [Ethical guidelines](#) still apply. In no event shall the Royal Society of Chemistry be held responsible for any errors or omissions in this *Accepted Manuscript* or any consequences arising from the use of any information it contains.

Cite this: DOI: 10.1039/c0xx00000x

www.rsc.org/xxxxxx

ARTICLE TYPE

Large-Scale Synthesis of PEGylated Lutetium Hydroxycarbonates as Nanoparticulate Contrast Agent for X-ray CT Imaging

Zhaogui Ba^{a,b}, Yumin Zhang^b, Junpei Wei^c, Jiwu Han^b, Zhenqiang Wang^b, Guangrui Shao^{a,*}^s Received (in XXX, XXX) Xth XXXXXXXXX 20XX, Accepted Xth XXXXXXXXX 20XX

DOI: 10.1039/b000000x

Nanoparticulate contrast agents have drawn considerable attention and interest because of their potential in medical diagnosis and prognosis. In the present study, we designed and constructed a high-performance nanoparticulate contrast agent based on PEGylated lutetium hydroxycarbonates (PEG-LuNPs) for X-ray computed tomography imaging, which was synthesized via a green and large-scale route. Under the daily clinical voltage, our PEG-LuNPs provided much more enhanced contrast than that of routinely used iodine-based molecules. More importantly, PEG-LuNPs could act as liver-targeted contrast agents for the further detection of hepatic metastases. Both in vitro and in vivo toxicity study indicated that these nanoparticles possessed extremely high biocompatibility, revealing their overall safety. Based on these results, PEG-LuNPs composed with intrinsic physicochemical property and excellent imaging capability demonstrated a useful nanoplatfrom for biomedical applications.

Introduction

Due to its cost effectiveness, deep tissue penetration, and high resolution, X-ray computed tomography (CT) has been regarded as one of the most powerful diagnostic imaging techniques along with the rapid development of modern medicine.¹⁻⁵ Small iodinated molecules are routinely used as CT contrast agents in the clinical setting. However, these contrast agents can effectively absorb X-rays but exhibit limitations due to rapid renal clearance, vascular permeation, and low specificity.⁶⁻¹⁰ Moreover, synthesis and purification of these iodine-based small molecules usually depend on multi-step methodologies. Thereby, the research focused on the development of novel CT contrast agents is essential.

Smart nano-engineered materials have moved into the spotlight as various high-resolution contrast agents owing to their excellent physicochemical property.¹¹⁻¹⁵ In particular, heavy metal-based nanoparticles can strongly absorb X-ray radiation and enhance imaging contrast by several folds even at low X-ray doses during the CT imaging.¹⁶⁻²⁰ Compared with small iodinated molecules, these nanoparticulate contrast agents possess a high contrast densities and a long blood circulation period, promising their in vivo targeted imaging and angiography.²¹⁻²³ In addition, these agents can display prominent superiority in imaging efficacy with respect to small iodinated molecules under clinical operating voltages ranging from 80 kVp to 140 kVp. More importantly,

these iodine-free nanoparticles can not result in an iodine-induced hypersensitivity reaction in clinic. Because a large amount of CT contrast agents is highly required during the imaging process, the following criteria must be cited with intense interest: (1) suitable X-ray attenuation coefficient under clinical operation; (2) high biocompatibility and low systemic toxicity; (3) cost effectiveness and facile synthesis. Among all currently available heavy metal-based nanomaterials, lanthanide-based particles hold great promise as CT contrast agents and have been used in CT imaging owing to their suitable K-edge energy located within the high-energy region of X-ray spectrum and high abundance in the earth.²⁴⁻²⁸ For example, lanthanide-doped NaYbF₄ nanoproboscopes were designed as the first Yb-based CT contrast agents for CT imaging.²⁹⁻³¹ Nanoparticles based on lanthanide oxide were prepared for multimodal imaging with extremely low systemic toxicity.³²⁻³⁴ Pro-drug-conjugated upconversion nanomaterials were used as multimodal imaging and NIR light-triggered anticancer treatment.³⁵ Although promising, there are still many intractable problems that hinder the development of this field, such as time-consuming and multi-step synthesis route to construct nanoparticulate contrast agents. More importantly, it is highly in demand to gain inexpensive and low-toxicity nano-CT contrast agents with facile and large-scale route.

Previous study has demonstrated that urea-based homogeneous precipitation method could act as a main route to prepare colloidal single-lanthanide hydroxycarbonates.³⁶ Very recently, Gd-doped Yb(OH)CO₃ nanoparticles have been constructed and applied as dual-modal contrast agents for X-ray computed tomography/magnetic resonance (CT/MR) imaging.³⁷ However, this direct synthesis without any surface modification can decrease the dissolvability of nanoparticulate contrast agents in physiological solution and hence cause serious aggregation

^a Department of Radiology, The Second Hospital of Shandong University, Shandong University, Jinan, Shandong 250033, P. R. China

Corresponding author: Guangrui Shao E-mail: shaoguangrui@yeah.net

^b Department of Radiology, Laigang Hospital Affiliated to Taishan Medical University, Laiwu, Shandong 271126, P. R. China

^c Department of Radiology, People's Hospital of Xintai City, Xintai, Shandong 271200, P. R. China

Z. G. Ba and Y. M. Zhang should be regarded as Joint First Authors.

occurred in animal body, indicating the inapplicability of these nanoagents in vivo. Inspired by above studies, a modified strategy based on urea-assistant homogeneous precipitation route was applied to prepare PEGylated Lu(OH)CO₃ nanoparticles (PEG-LuNPs) by doping polyethylene glycol molecules (PEG) in the synthesis process. With extremely low cytotoxicity and hemolysis, these contrast agents exhibited excellent efficiency in CT imaging with respect to small iodinated molecules. Otherwise, PEG-LuNPs could be effectively accumulated into the liver of experimental animals and act as a liver-targeted contrast agent, promising for the further detection of hepatic metastases. Long-term toxicity studies including body weight analysis, histology assay, and blood biochemistry assay were also carried out after a single-dose intravenous injection in a mouse model, revealing the overall safety of our well-prepared contrast agents.

Experimental section

Materials

Lutetium chloride hexahydrate (LuCl₃·6H₂O), chloral hydrate, polyethylene glycol (PEG-2000) and urea were obtained from Aladdin Reagent. Iobitridol was purchased from Guerbet. Other reagents and solvents were acquired from Beijing Chemicals.

Preparation of PEGylated Lu(OH)CO₃ nanoparticles

PEGylated Lu(OH)CO₃ nanoparticles were prepared via a one-pot urea-based homogeneous precipitation process. Typically, LuCl₃·6H₂O (6.0 mmol), PEG-2000 (2.0 g), and urea (200 mmol) were dissolved in deionized water (400 mL). After magnetic stirring at room temperature for 2 h, the resultant homogeneous solution was reacted at 90 °C for another 3 h. The product was collected after washing with deionized water and ethanol in sequence, and dried in vacuum at 60 °C overnight for further use.

Cell cultures

Hela cells were supplied by American Type Culture Collection. Cells were cultured in Dulbecco's modified Eagle's medium (DMEM) containing streptomycin (100 U mL⁻¹), 10% fetal bovine serum (FBS) and penicillin (100 U mL⁻¹), in a humidified incubator at 37 °C and 5% CO₂. The cells were harvested by the use of trypsin and were re-put back into fresh complete medium before plating.

In vitro cytotoxicity studies

To quantify the cytotoxicity of PEG-LuNPs, MTT assays were carried out. Hela cells were cultured in 96-well plates at a density of 5×10³ per well for 12 h to allow the cells to attach. Serial dilutions of different agent formulations were added to the culture medium. One day later, the medium containing PEG-LuNPs were removed, and cell samples were treated with MTT for another 4 h. dimethyl sulfoxide (DMSO) was used to dissolve the formazan crystals. Six replicates were done in each group and the percent viability was normalized to the cell viability without treatment.

Observation of cellular modality

Hela cells with a density of 2×10⁴ were plated in a 12-well plate for 6 h to allow the cells to attach. PEG-LuNPs (0.4 mg mL⁻¹) was added to the cell culture medium. After 24 h of incubation,

cells were washed several times with 0.9% NaCl to remove the remaining nanoparticles, stained with trypan blue, and then observed under an optical microscopy.

In vitro hemolysis assay

The hemolysis assay experiments were performed evaluate the in vitro biocompatibility. Blood sample (1 mL) was added into 0.9% NaCl (3 mL), and then red blood cells (RBCs) were isolated from serum by centrifugation. After being washed several times with 0.9% NaCl, the purified blood was diluted to 1/10 of its volume with 0.9% NaCl. Diluted RBC suspension (0.2 mL) was then mixed with (a) 0.9% NaCl (0.8 mL) as a negative control, (b) D. I. water (0.8 mL) as a positive control, and (c) suspensions (0.8 mL) of PEG-LuNPs with concentrations ranging from 0 to 1 mg mL⁻¹. All the mixtures were vortexed and kept at room temperature for 3 h. Finally, the mixtures were centrifuged, and the absorbance of supernatants at 541 nm was determined through UV-vis-NIR spectrophotometer.

Animal administration

Wister rats, Kunming mice, and C57BL/6 mice were obtained from Laboratory Animal Center of Shandong University (Jinan, China). There handling and care procedures were under the jurisdiction and guidelines of the Regional Ethics Committee for Animal Experiments.

Establishment of tumour-bearing model

A subcutaneous transplantable mouse model of lung cancer was prepared via injecting Lewis lung carcinoma cells (1×10⁶) in 0.9% NaCl (0.1 mL) at the right axillary fossa of C57BL/6 mice.

CT imaging

To assess CT contrast efficacy, PEG-LuNPs and Iobitridol were dispersed in NaCl containing 1% agarose with different Lu and I concentrations. The Eppendorf tubes were scanned in a Philips CT imaging system. For in vivo imaging, rats were firstly anesthetized by intraperitoneally injecting chloral hydrate (10 wt%). PEG-LuNPs in 0.9% NaCl (100 mg kg⁻¹) was injected intravenously. CT images were then acquired using a Philips Medical System. The clinical operation voltage was denoted as 120 kVp.

Change in body weight

Kunming mice were separated into two cages (n = 6). The mice in test group were injected intravenously with PEG-LuNPs (200 mg kg⁻¹). In addition, mice injected with 0.9% NaCl were selected as control group. We recorded the change in body weight for a month.

Assay of histology and blood biochemistry

All the mice in both groups were sacrificed a month later. Main exposed organs including heart, liver, spleen, lung, and kidney were collected. These organs were then fixed at 10% neutral buffered formalin, embedded in paraffin, sectioned (4 μm thick), and stained with hematoxylin and eosin (H&E). The histological sections were observed under an optical microscope. Otherwise, blood from above groups was collected to carry out blood biochemical assay.

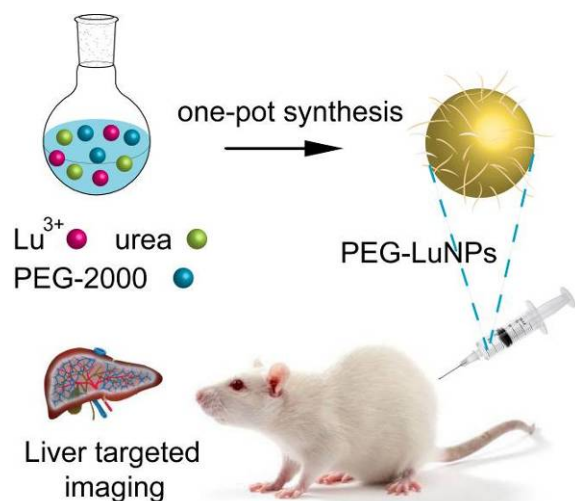


Fig. 1. Schematic illustration for the synthesis of PEG-LuNPs and their application as X-ray CT contrast agents.

5 Results and discussion

Synthesis and characterisation of PEGylated Lu(OH)CO₃ nanoparticles

Fig. 1 clearly illustrated our design and synthesis of PEGylated Lu(OH)CO₃ nanoparticles, as well as their application as X-ray CT contrast agents. Typical construction of PEG-LuNPs was performed via a modified urea-based homogeneous precipitation method by doping PEG molecules in the synthesis process. Due to the self decomposition of urea into OH⁻ and CO₃²⁻ at high temperature, this classical method has been considered as a general route for the preparation of lanthanide hydroxylcarbonate. By doping PEG molecules, our nanoparticulate contrast agents could dispersed well in various physiological solution. SEM image and TEM image shown in Fig. 2A and Fig. 2B revealed that our PEG-LuNPs presented a non-aggregated and spherical nature with a smooth surface. Particle-size distribution obtained

from TEM result shown in Figure 3C indicated that PEG-LuNPs had a mean diameter of 115 nm. To test the accurate hydrodynamic size of PEG-LuNPs, dynamic light scattering (DLS) was further carried out, indicating the well-prepared nanoparticles had an average diameter of 135 nm with a standard deviation of ± 21.4 nm. Energy-dispersive spectroscopy (EDS) analysis via the point scan mode revealed the presence of Lu, C, and O elements in PEG-LuNPs (Fig. 2D). FT-IR revealed the characteristic adsorption bands of VasO-C-O (1530 and 1406 cm⁻¹), π -CO₃²⁻ (844 cm⁻¹), and δ -CO₃²⁻ (762 and 696 cm⁻¹), which was in accordance with carbonate group (Fig. 2E).³⁷ Otherwise, the bands around 3000 cm⁻¹ in the spectrum was assigned to C-H stretching vibration, indicating the successful modification of PEG molecules on the surface of nanoparticles.³⁸ Considering that a large amount of CT contrast agents are highly required in clinic, large-scale production of nanoagents must be achieved via a facile process. As illustrated in Fig. 2F, the large-scale production of PEG-LuNPs could be easily obtained via increasing the amount of reagents and the product exhibited a white color. Compared with previous studies, our present method was free of organic reagents and showed a facile fabrication route.

In vitro toxicity

From the viewpoint of diagnosis and prognosis in clinical setting, contrast agents must be non-toxic and biocompatible. Although nanoparticles based on lanthanide hydroxylcarbonate are well known to be low cytotoxicity, we also carried out a methyl thiazolyl tetrazolium (MTT) assay to test the cytotoxicity of PEG-LuNPs, which must be established before small-animal experiments. One day after being exposed to PEG-LuNPs with various concentrations, results of viability of Hela cells exhibited that more than 90% cells survived (Fig. 3A). With the presence of our nanoparticulate contrast agents with a concentration of 0.4 mg mL⁻¹, microscopy images of Hela cells illustrated no obvious difference in the cell morphology for the cells treated with PEG-LuNPs compared to the control group (Fig. 3B). Hemolytic assay

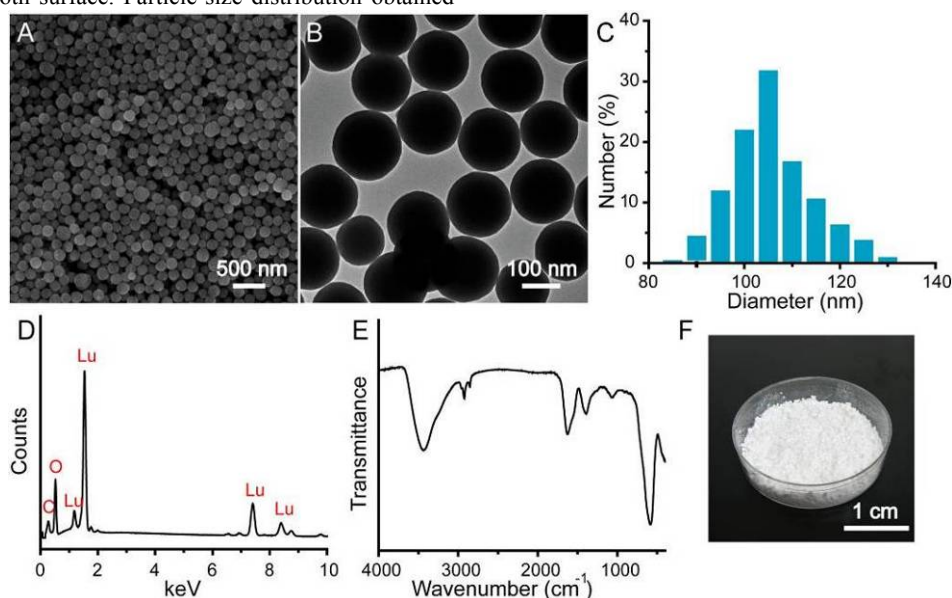


Fig. 2. SEM image (A), TEM image (B), size distribution (C), EDS spectrum (D), FT-IR spectra (E), and large-scale production (F) of PEG-LuNPs. The total synthesis volume of solution was denoted as 500 mL.

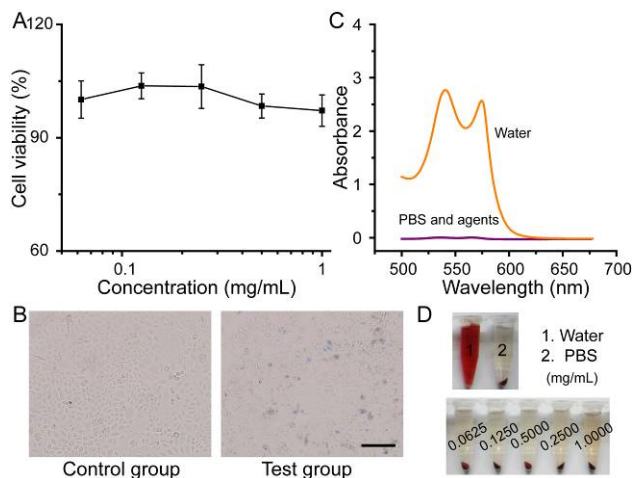


Fig. 3. Effect of PEG-LuNPs on the viability of HeLa cells (A). Optical microscopy images of trypan blue stained cells (B). Effect of PEG-LuNPs on the red cells (C). Photographic images for direct observation of hemolysis (D). The black scale bar represented 100 μm .

was additionally used to evaluate the blood compatibility.^{39, 40} UV-vis spectrum and photographic images further demonstrated that PEG-LuNPs caused no hemolysis of RBCs even upon the maximal experimental concentration (1 mg mL^{-1}). On the basis of these results, it could be inferred that PEG-LuNPs was highly compatible towards both HeLa cells and RBCs, thus implying that PEG-LuNPs could serve as a safe CT contrast agent for in vivo CT imaging.

CT imaging

In preliminary in vivo animal experiments, we first examined the contrast efficiency of PEG-LuNPs relative to iobitridol (a popular

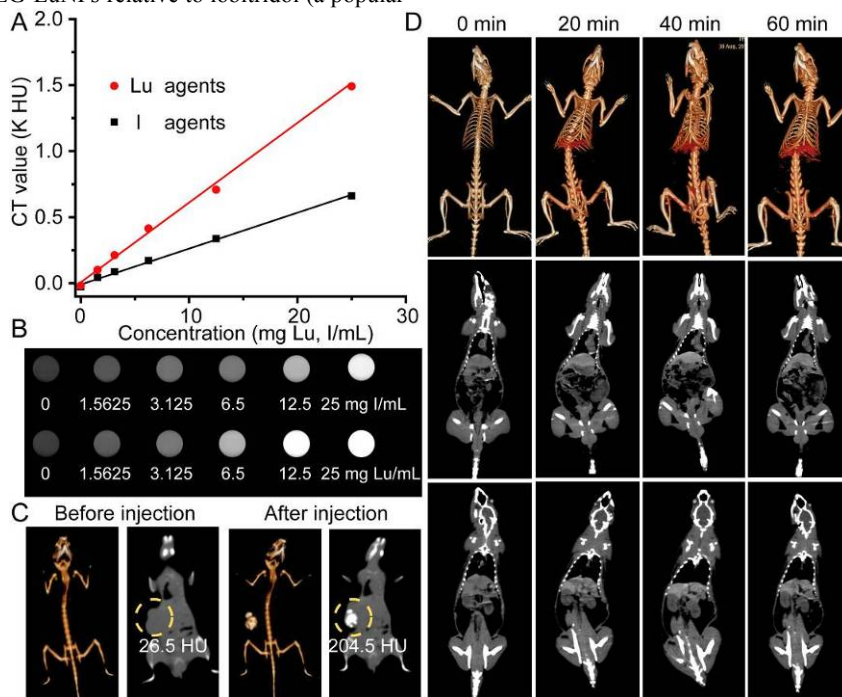


Fig. 4. CT value (A) and In vitro CT images (B) of PEG-LuNPs and Iobitridol. CT images of a tumour-bearing C57BL/6 mouse before and after intratumoral injection (C). In vivo CT view images of rats after intravenous injection of PEG-LuNPs.

iodine-based X-ray CT contrast agent in clinic). Fig. 4A and Fig. 4B displayed that both contrast agents exhibited signal enhancement with the increase of contrast agent concentration, and samples containing higher concentration of contrast agents appeared brighter on CT images. A good linear correlation between the Hounsfield units (HU) value and the concentration of Lu or I was observed at the same time. Notably, the obtained HU values of PEG-LuNPs were significantly enhanced compared to iobitridol at equivalent concentration of each agent. These results implied that our PEG-LuNPs might be applied with a reduced dosage, thus lowering the possible adverse side effects. Having established high biocompatibility and high contrast efficiency, in vivo CT imaging studies with PEG-LuNPs were next performed on a clinical CT system. Owing to the high atomic number and electron density of lanthanon elements, PEG-LuNPs could result in enhanced positive contrast around the injection sites than other soft tissue. For primary in vivo CT imaging, PEG-LuNPs were intratumourally injected into a tumour-bearing mouse. Fig. 4C revealed an obvious enhancement of CT signal around the tumour site after injection. Encouraged by our above results, we further evaluated the whole body CT imaging by intravenous injection of PEG-LuNPs and assessed the biodistribution of contrast agents tracked by clinical CT system. The rat was anesthetized at first and injected intravenously with PEG-LuNPs dispersion in 0.9% NaCl solution. Fig. 4D presented the coronal view and 3D-renderings CT images of the rat. Once solution containing PEG-LuNPs was injected, a clear signal enhancement of the liver was observed at an early time (20 min). Remarkably, the gradual signal enhancement of liver and spleen continued for over 60 min. More careful look via 3D-renderings of CT images also provided evident signal enhancement of liver vessel. According to above

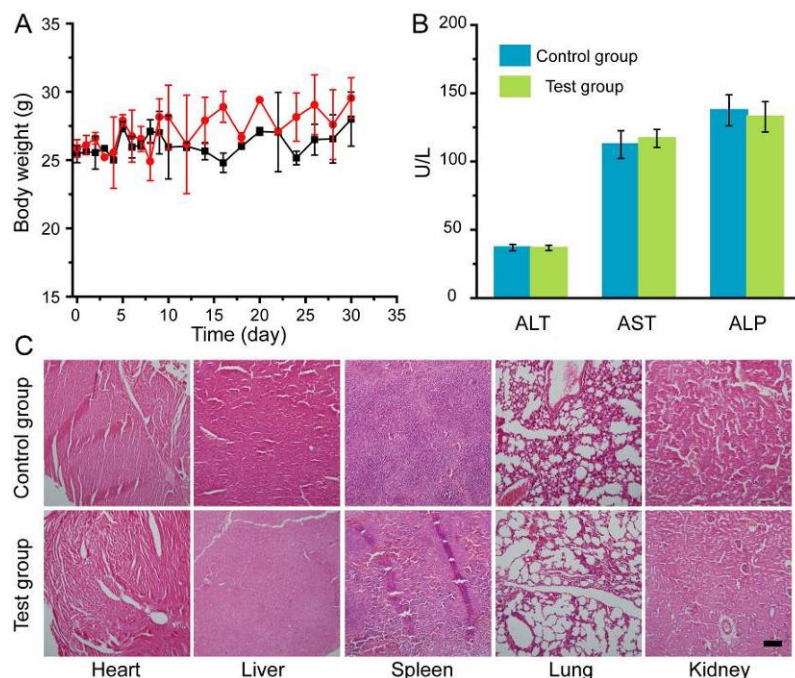


Fig. 5. Body weight change (A), blood biochemical assay (B), and main-organ histological changes of mice a month after intravenous injection of PEG-LuNPs and 0.9 % NaCl solution. The black scale bar represented 100 μm.

results, our PEG-LuNPs could act as high-performance a liver-targeted CT contrast agent. Compared with small iodinated molecules, PEG-LuNPs decorated with anti-biofouling polymer could prolong their blood circulation period and overcome the limitation in targeted imaging and angiography. Different from normal tissue, tumour tissue can uptake more contrast agents during the imaging process owing to the intrinsic enhanced permeation and retention effect (EPR).^{7, 21, 27} More importantly, our PEG-LuNPs accumulated in liver could serve as a useful CT contrast agent for the detection of hepatic metastases.

Investigation of Long-term toxicity

Last but not least, we tested the long-term toxicity of PEG-LuNPs. After intravenous injection of a single dose of PEG-LuNPs, all the mice remained healthy over a one-month period. No abnormalities in eating, drinking, activity, exploratory behaviour, or neurological status were noticed at the same time.⁴¹⁻⁴⁶ As shown in Fig. 5A, body weight of test group increased slightly in a pattern similar to that of control group. One month after injection, several important hepatic indicators such as alanine transaminase (ALT), aspartate transaminase (AST), and alkaline phosphatase (ALP) were selected to carry out blood biochemical assay. All the measured parameters fell within the normal ranges and revealed no sign of liver injury (Fig. 5B). Mice in both groups were then sacrificed for careful necropsy. To determine whether these nanoparticles caused any tissue damages or any other toxic effect on mice, major organs including heart, liver, spleen, lung, and kidney were sliced and stained by hematoxylin and eosin (H&E) for histological assessment. Fig. 5C revealed that no noticeable tissue damages or any other toxic effect on organs occurred. However, many careful studies are still needed to examine the potential toxicity of PEG-LuNPs with a much

longer term, which is significant for the further application of this type of nanoparticulate contrast agents in biomedicine.

Conclusions

In summary, we reported here a facile strategy to synthesize monodispersed X-ray CT contrast agents based on PEGylated lutetium hydroxycarbonates nanoparticles via a modified urea-based homogeneous precipitation method by doping PEG molecules. Detailed evaluation of cytotoxicity and hemolysis demonstrated the excellent biocompatibility and extremely low cytotoxicity of our PEGylated Lu(OH)CO₃ nanoparticles. Compared with routinely used Iobitridol in clinic, our nanoparticulate contrast agents could provide much obvious enhancement upon clinical voltages. More importantly, this liver-targeted CT contrast agent presented more potential in further detection of hepatic metastases due to its efficient accumulation in liver after intravenous injection. In addition, long-term toxicity study indicated that our well-prepared nanoparticulate CT contrast agents processed overall safety and promised for further biomedical usages.

References

- 1 T. Skotland, *Contrast Media Mol. Imaging* 2012, **7**, 1.
- 2 S. Yu and A. Watson, *Chem. Rev.* 1999, **99**, 2353.
- 3 J. Kim, Y. Piao and T. Hyeon, *Chem. Soc. Rev.* 2009, **38**, 372.
- 4 G. Maltzahn, J. Park, A. Agrawal, N. Bandaru, S. Das, M. Sailor and S. Bhatia, *Cancer Res.* 2009, **69**, 3892.
- 5 W. Cai and X. Chen, *Small* 2007, **3**, 1840.
- 6 A. Jakhmola, N. Anton, T. Vandamme, *Adv. Healthcare Mater.* 2012, **1**, 413.

- 7 H. Wang, L. Zheng, C. Peng, R. Guo, M. Shen, X. Shi and G. Zhang, *Biomaterials* 2011, **32**, 2979.
- 8 M. Shilo, T. Reuveni, M. Motiei and R. Popovtzer, *Nanomedicine-UK* 2012, **7**, 257.
- 5 9 S. Zeng, M. Tsang, C. Chan, K. Wong and J. Hao, *Biomaterials* 2012, **33**, 9232.
- 10 J. Zhou, M. Yu, Y. Sun, X. Zhang, X. Zhu, Z. Wu, D. Wu and F. Li, *Biomaterials* 2011, **3**, 1148.
- 11 K. Park, S. Lee, E. Kang, K. Kim, K. Choi and I. Kwon, *Adv. Funct. Mater.* 2009, **19**, 1553.
- 10 12 L. Cheng, K. Yang, S. Zhang, M. Shao, S. Lee and Z. Liu, *Nano Res.* 2010, **3**, 722.
- 13 G. Tian, Z. Gu, L. Zhou, W. Yin, X. Liu, L. Yan, S. Jin, W. Ren, G. Xing, S. Li and Y. Zhao, *Adv. Mater.* 2012, **24**, 1226.
- 15 14 Y. Wang, H. Wang, D. Liu, S. Song, X. Wang, and H. Zhang, *Biomaterials* 2013, **34**, 7715.
- 15 M. Oh, N. Lee, H. Kim, S. Park, Y. Piao, J. Lee, S. Jun, W. Moon, S. Choi, and T. Hyeon, *J. Am. Chem. Soc.* 2011, **133**, 5508.
- 20 16 C. Alric, J. Taleb, G. Duc, C. Mandon, C. Billotey, A. Meur-Herland, T. Brochard, F. Vocanson, M. Janier, P. Perriat, S. Roux and O. Tillement, *J. Am. Chem. Soc.* 2008, **130**, 5908.
- 25 17 Q. Yin, F. Yap, L. Yin, L. Ma, Q. Zhou, L. Dobrucki, T. Fan, R. Gaba, and J. Cheng, *J. Am. Chem. Soc.* 2013, **135**, 13620.
- 18 A. Xia, Y. Gao, J. Zhou, C. Li, T. Yang, D. Wu, L. Wu and F. Li, *Biomaterials* 2011, **32**, 7200.
- 30 19 D. Pan, C. Schirra, A. Senpan, A. Schmieder, A. Stacy, E. Roessl, A. Thran, S. Wichline, R. Proska and G. Lanza, *ACS Nano* 2012, **6**, 3364.
- 20 Z. Liu, F. Pu, J. Liu, L. Jiang, Q. Yuan, Z. Li, J. Ren and X. Qu, *Nanoscale* 2013, **5**, 4252.
- 35 21 X. Zhu, J. Zhou, M. Chen, M. Shi, W. Feng and F. Li, *Biomaterials* 2012, **33**, 4618.
- 22 K. deKrafft, W. Boyle, L. Burk, O. Zhou, and W. Lin, *J. Mater. Chem.* 2012, **22**, 18139.
- 23 H. Xing, W. Bu, Q. Ren, X. Zheng, M. Li, S. Zhang, H. Qu, Z. Wang, Y. Hua, K. Zhao, L. Zhou, W. Peng and J. Shi, *Biomaterials* 2012, **33**, 5384.
- 40 24 D. Pan, C. Schirra, S. Wickline, and G. Lanza, *Contrast Media Mol. Imaging* 2014, **9**, 13.
- 25 Y. Wu, Y. Sun, X. Zhu, Q. Liu, T. Cao, J. Peng, Y. Yang, W. Feng, and F. Li, *Biomaterials* 2014, **35**, 4699.
- 45 26 M. He, P. Huang, C. Zhang, H. Hu, C. Bao, G. Gao, R. He, and D. Cui, *Adv. Funct. Mater.* 2011, **21**, 4470.
- 27 Q. Xiao, X. Zheng, W. Bu, W. Ge, S. Zhang, F. Chen, H. Xing, Q. Ren, W. Fan, K. Zhao, Y. Hua, and J. Shi, *J. Am. Chem. Soc.* 2013, **135**, 13041.
- 50 28 D. Yang, Y. Dai, J. Liu, Y. Zhou, Y. Chen, C. Li, P. Ma, and J. Lin, *Biomaterials* 2014, **35**, 2011.
- 29 Y. Liu, K. Ai, J. Liu, Q. Yuan, Y. He and L. Lu, *Angew. Chem. Int. Ed.* 2012, **51**, 1437.
- 55 30 Y. Liu, K. Ai, J. Liu, Q. Yuan, Y. He, and L. Lu, *Adv. Healthcare Mater.* 2012, **1**, 461.
- 31 Y. Liu, K. Ai, and L. Lu, *Acc. Chem. Res.* 2012; **45**: 1817.
- 32 Z. Liu, Z. Li, J. Liu, S. Gu, Q. Yuan, J. Ren, and X. Qu, *Biomaterials* 2012, **33**, 6748.
- 60 33 Z. Liu, F. Pu, S. Huang, Q. Yuan, J. Ren and X. Qu, *Biomaterials* 2013, **34**, 1712.
- 34 Z. Liu, K. Dong, J. Liu, X. Han, J. Ren, and X. Qu, *Small*, 2014, **10**, 2429.
- 35 Y. Dai, H. Xiao, J. Liu, Q. Yuan, P. Ma, D. Yang, C. Li, Z. Cheng, Z. Hou, P. Yang, and J. Lin, *J. Am. Chem. Soc.* 2013, **135**, 18920.
- 65 36 E. Matijevic and W. Hsu, *J Colloid Interface Sci* 1987, **118**, 506.
- 37 Y. Jin, J. Liu, Q. Zheng, J. Xu, B. Sharma, G. He, M. Yin, L. Zhang, Y. Song, T. Li, Q. Yuan, Y. Sun, and H. Yang, *New J. Chem.* 2013, **37**, 3024.
- 70 38 Z. Yue, W. Wei, Z. You, Q. Yang, H. Yue, Z. Su, and G. Ma, *Adv. Funct. Mater.* 2011, **21**, 3446.
- 39 I. Slowing, C. Wu, J. Vivero-Escoto and V. Lin, *Small* 2009, **5**, 4834.
- 75 40 Y. Lin and C. Haynes, *J. Am. Chem. Soc.* 2010, **132**, 4834.
- 41 L. Cheng, K. Yang, M. Shao, X. Lu and Z. Liu, *Nanomedicine-UK* 2011, **6**, 1327.
- 42 Y. Liu, K. Ai, J. Liu, M. Deng, Y. He, and L. Lu, *Adv. Mater.* 2013, **25**, 1353.
- 80 43 C. Peng, L. Zheng, Q. Chen, M. Shen, R. Guo, H. Wang, X. Cao, G. Zhang, and X. Shi, *Biomaterials* 2012, **33**, 1107.
- 44 R. Guo, H. Wang, C. Peng, M. Shen, L. Zheng, G. Zhang, and X. Shi, *J. Mater. Chem.* 2011, **21**, 5120.
- 85 45 Y. Fang, C. Peng, R. Guo, L. Zheng, J. Qin, B. Zhou, M. Shen, X. Lu, G. Zhang, and X. Shi, *Analyst* 2013, **138**, 3172.
- 46 H. Liu, H. Wang, Y. Xu, M. Shen, J. Zhao, G. Zhang, and X. Shi, *Nanoscale* 2014, **6**, 4521.